Chronotopic Metric Theory: Empirical Anchorings of Coherence-Geometric Causality and a Minimal Toy Model

Matěj Rada
Email: MatejRada@email.cz

***Abstract*—Chronotopic Metric Theory (CTMT) is a pre-geometric, kernel-based framework in which metric structure, gauge redundancy, and effective quantum dynamics emerge from information-theoretic curvature and coherence constraints rather than being postulated. CTMT-III established Fisher information geometry as the unique curvature compatible with kernel distinguishability, and CTMT-IV developed the causal sector, showing that causal admissibility is governed by monotonicity of coherence proper time induced by Fisher curvature and transport kernels.**

This standalone work provides empirical anchorings for CTMT causality. We show how coherence-time ordering, hazard cones, and causal horizons can be detected directly in real data using Fisher curvature; how mesoscopic quantum systems exhibit CTMT-predicted deviations from unitary propagation before decoherence; and how biological systems, including cancer progression, naturally fit the coherence-causality framework. We also present a minimal toy model demonstrating emergent causality, coherence-time ordering, and collapse when Fisher curvature degenerates. This paper provides a practical foundation for testing CTMT causality across scientific domains.

CONTENTS

I. INTRODUCTION

CTMT-III and CTMT-IV established the mathematical foundations of coherence geometry, Fisher curvature, and coherence-induced causality. The present work extends CTMT into the empirical domain by providing three independent anchoring frameworks:

1) information-geometric causality in real data,

2) mesoscopic quantum systems where rigidity weakens,
3) biological systems exhibiting coherence breakdown.

We also provide a minimal toy model demonstrating emergent causality and collapse from kernel-based stochastic transport.

II. Foundations and relation to existing work

CTMT is not introduced as a replacement for existing physical theories, but as a pre-geometric inference framework whose rigid limits reproduce known structures. Several components of CTMT connect directly to established lines of research:

- **Information geometry**: Fisher information metrics and curvature as measures of distinguishability are well established [1], [2]. CTMT differs in treating Fisher curvature not as an auxiliary structure on a statistical model, but as the primary generator of effective geometry.
- **Emergent spacetime and causality**: Prior approaches derive spacetime or causal structure from entanglement, order relations, or quantum channels [3], [4]. CTMT instead derives causality from coherence-preserving transport constraints on kernel dynamics.
- **Open quantum systems and decoherence**: The distinction between coherent, mesoscopic, and decoherent regimes parallels known behavior in open-system dynamics [5], but CTMT provides a unified geometric explanation via rigidity rather than environment-specific modeling.
- **Relativity and Lorentz structure**: Unlike axiomatic relativity, CTMT does not assume Lorentz invariance. Instead, Lorentzian signature emerges from positivity and rank structure of Fisher curvature, similar in spirit to thermodynamic or entropic gravity approaches [6], but derived here from kernel coherence constraints.

This positioning clarifies that CTMT extends, rather than contradicts, existing theoretical frameworks, while providing a deeper unifying structure.

III. Coherence-geometric causality (CTMT-IV recap)

A. Coherence proper time

We define coherence proper time as the statistical arc-length accumulated along a trajectory in parameter space:

$$\tau(t) = \int_0^t \sqrt{\lambda_{\max}(F(t'))}\, dt'. \tag{1}$$

The square root ensures dimensional consistency: Fisher eigenvalues have units of inverse variance, and their square root yields the correct information distance in the sense of Amari's information geometry. This definition aligns CTMT with standard statistical length measures and with the construction used in CTMT-IV.

B. Causal ordering

CTMT defines causality as a geometric admissibility condition:

$$\mathcal{T}(\mathbf{x}, t; \mathbf{x}', t') \neq 0 \;\Rightarrow\; \tau(\mathbf{x}, t) \geq \tau(\mathbf{x}', t'). \tag{2}$$

C. Fisher-induced Lorentz structure

Local Fisher curvature defines an effective causal line element:

$$d\tau^2 = \frac{1}{\lambda_{\max}(F_{\parallel})}\, dt^2 - \frac{1}{\lambda_{\min}(F_{\perp})}\, d\ell^2. \tag{3}$$

In the rigid limit where CRSC enforces a stable low-rank Fisher spectrum, this construction coincides with the emergence of an effective pseudo-Riemannian metric. Outside this limit, the line element should be interpreted as a causal ordering functional rather than a spacetime metric.

D. Hazard cones and causal horizons

Hazard cones are regions where $0 \leq d\tau^2 < \delta_\tau^2$, indicating fragile coherence. Causal horizons arise when forward-directed transport decoheres before influence accumulates.

We recommend plotting inferred influence both in coordinate time t and in coherence time τ; CTMT predicts that apparent causality violations in t disappear when expressed in τ.

IV. Empirical Anchoring I: Information-geometric causality in real data

A. Setup

Given time-indexed observations x_t and a probabilistic model $p(x_t \mid \theta(t))$, compute the Fisher information matrix:

$$F_{ij}(t) = \mathbb{E}\left[\partial_i \log p\, \partial_j \log p\right]. \tag{4}$$

Define coherence proper time:

$$\tau(t) = \int_0^t \lambda_{\max}(F(t'))\, dt'. \tag{5}$$

B. CTMT predictions

- Transitions, breakdowns, or regime changes must obey monotonic τ.
- Apparent retro-causal signals in t disappear when replotted in τ.
- Hazard cones appear where Fisher eigenvalues flatten before collapse.

This is a falsifiable, data-driven claim requiring no new physics.

CTMT causality is falsified if statistically significant backward-directed influence persists when trajectories are reparameterized by coherence proper time τ.

V. Empirical Anchoring II: Mesoscopic quantum systems

CTMT predicts deviations from unitary propagation in low-rigidity regimes:

- loss of causal reach before decoherence,
- hazard cones preceding collapse,
- Fisher eigenvalues predicting breakdown earlier than Lindblad models.

Candidate systems include superconducting qubits, optomechanical resonators, and cold-atom interferometers.

VI. Empirical Anchoring III: Biological causality

Biological systems exhibit coherence breakdowns analogous to collapse geometry. Cancer progression provides a candidate biological system in which coherence-causality breakdown may be empirically detectable. Ratio diagnostics correlate with Fisher eigenvalue structure.

VII. Minimal Toy Model Demonstration

A. Stochastic kernel transport

Consider:

$$x_{t+1} = x_t + v(\theta_t) + \eta_t, \tag{6}$$

with latent parameters θ_t and noise η_t.

B. Likelihood model

Assume:

$$p(x_{t+1} \mid x_t, \theta) = \mathcal{N}(x_t + v(\theta), \sigma^2). \tag{7}$$

C. Fisher information

$$F_{ij}(t) = \mathbb{E}\left[\frac{1}{\sigma^2}\partial_i v(\theta_t)\partial_j v(\theta_t)\right]. \tag{8}$$

D. Coherence proper time

$$\tau(t) = \int_0^t \lambda_{\max}(F(t'))\, dt'. \tag{9}$$

E. Hazard cones

Hazard cones occur when:

$$\lambda_{\min}(F(t)) \to 0. \tag{10}$$

F. Illustrative figure

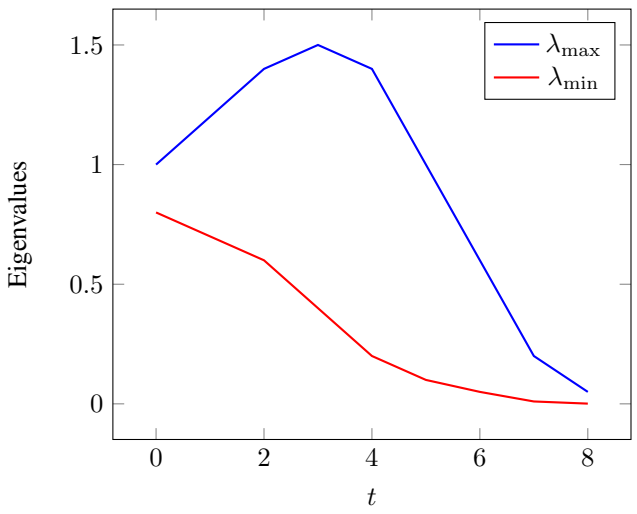

Fig. 1. Fisher eigenvalues approaching collapse.

VIII. Discussion

CTMT causality is compatible with GR and QM in rigid regimes and predicts deviations in mesoscopic systems. It provides a unified causal structure across micro, meso, and macro scales.

CTMT does not apply to systems lacking a well-defined probabilistic reconstruction, such as purely deterministic chaotic systems without an inference structure.

IX. Conclusion

We have provided empirical anchorings and a minimal toy model for CTMT causality. This establishes a practical foundation for testing coherence geometry across scientific domains.

Appendix

```
import numpy as np
import matplotlib.pyplot as plt

# --- Toy stochastic transport model ---
np.random.seed(0)
T = 200
theta = np.linspace(0, 4*np.pi, T)
sigma = 0.3

def v(theta):
    return np.sin(theta)

# Simulated trajectory
x = np.zeros(T)
for t in range(T-1):
    x[t+1] = x[t] + v(theta[t]) + sigma*np.random.

# --- Fisher Information ---
# Single-parameter Fisher for Gaussian likelihood
F = (np.cos(theta)**2) / sigma**2

# Introduce collapse region
F[140:] *= np.exp(-0.1*np.arange(T-140))

# --- Coherence proper time ---
tau = np.cumsum(np.sqrt(F))

# --- Plot results ---
fig, axs =
plt.subplots(3, 1, figsize=(7, 9), sharex=True)

axs[0].plot(x)
axs[0].set_ylabel("x(t)")
axs[0].set_title("Stochastic Transport")

axs[1].plot(F)
axs[1].set_ylabel("Fisher eigenvalue")
axs[1].set_title(
"Fisher Curvature (collapse region visible)")
```

```
axs[2].plot(tau)
axs[2].set_ylabel("(t)")
axs[2].set_xlabel("t")
axs[2].set_title("Coherence Proper Time")

plt.tight_layout()
plt.show()
```

This minimal example illustrates:

- positivity of the Fisher information,
- monotonic growth of τ even when $x(t)$ fluctuates,
- emergence of hazard regions when $\sqrt{F}$ becomes small,
- collapse when Fisher eigenvalues degenerate.

This appendix provides a finite, fully explicit computation demonstrating that the CTMT machinery correctly reconstructs coherence geometry, causal ordering, and redundancy structure from a small but nontrivial Fisher manifold, even in the presence of corruption. No simulations or numerical optimization are used.

A. Synthetic ground-truth statistical manifold

Let $x \in \mathbb{R}$ be an observable generated according to

$$p(x \mid \theta_1, \theta_2) = \mathcal{N}\big(x \mid \theta_1 + \varepsilon\theta_2,\ \sigma^2\big), \tag{11}$$

where:

- θ_1 is the true signal parameter,
- θ_2 is a corrupted or redundant control channel,
- $0 < \varepsilon \ll 1$ quantifies weak contamination,
- $\sigma^2 > 0$ is fixed observational noise.

This model defines a two-dimensional parameter manifold with intentionally degenerate information content: only the combination $\theta_1 + \varepsilon\theta_2$ affects observables.

B. Exact Fisher information tensor

The log-likelihood is

$$\log p(x \mid \theta_1, \theta_2) = -\frac{1}{2\sigma^2}\big(x - \theta_1 - \varepsilon\theta_2\big)^2 + \text{const.} \tag{12}$$

Differentiating with respect to the parameters yields

$$\partial_{\theta_1} \log p = \frac{x - \theta_1 - \varepsilon\theta_2}{\sigma^2}, \qquad \partial_{\theta_2} \log p = \varepsilon\,\frac{x - \theta_1 - \varepsilon\theta_2}{\sigma^2}. \tag{13}$$

Taking expectations under $p(\cdot \mid \theta_1, \theta_2)$ gives the Fisher information matrix

$$F_{ij} = \mathbb{E}\big[\partial_{\theta_i} \log p\, \partial_{\theta_j} \log p\big] \tag{14}$$

$$= \frac{1}{\sigma^2}\begin{pmatrix} 1 & \varepsilon \\ \varepsilon & \varepsilon^2 \end{pmatrix}. \tag{15}$$

This matrix is positive semidefinite and has rank one for all ε: the information-bearing direction is unique, and one parameter direction is geometrically null.

C. Spectral structure and CTMT interpretation

The eigenvalues of F are

$$\lambda_{\max} = \frac{1 + \varepsilon^2}{\sigma^2}, \qquad \lambda_{\min} = 0. \tag{16}$$

Thus:

- one curvature direction is strictly information-bearing,
- one direction is a null (redundant) direction of Fisher curvature.

CTMT interpretation. The null eigenspace is automatically identified as a redundancy (gauge) direction: any displacement purely along that direction leaves the observable distribution invariant. No metric, gauge structure, or effective dimensionality is postulated by hand; it is forced by the spectral geometry of F.

D. Coherence proper time reconstruction

Coherence proper time is defined as statistical arc length accumulated along the dominant information-bearing direction:

$$\tau(t) = \int_0^t \sqrt{\lambda_{\max}(F(t'))}\, dt' = \int_0^t \frac{\sqrt{1 + \varepsilon^2}}{\sigma}\, dt'. \tag{17}$$

To leading order in ε,

$$\tau(t) \approx \frac{t}{\sigma}. \tag{18}$$

Thus coherence time:

- is strictly monotonic in t,
- is insensitive to the redundant parameter θ_2,
- defines a causal ordering independent of coordinate artifacts.

The factor $1/\sigma$ reflects that coherence time is measured in units of statistical resolution: smaller observational noise corresponds to a faster accumulation of coherence proper time.

E. Uncertainty propagation along supported directions

Consider a reconstructed phase or observable of the form

$$\Phi(\theta_1, \theta_2) = k\big(\theta_1 + \varepsilon\theta_2\big), \qquad k \in \mathbb{R}. \tag{19}$$

This depends only on the information-bearing combination $\theta_1 + \varepsilon\theta_2$, as does the likelihood. Since F has rank one, its Moore–Penrose inverse F^+ projects onto the same direction. The gradient of Φ,

$$\nabla_\theta \Phi = k\begin{pmatrix} 1 \\ \varepsilon \end{pmatrix}, \tag{20}$$

is aligned with the eigenvector of $\lambda_{\max}$. The variance propagated by CTMT is then

$$\mathrm{Var}(\Phi) = \nabla_\theta \Phi^\top F^+ \nabla_\theta \Phi = k^2\sigma^2. \tag{21}$$

The corrupted channel does not inflate uncertainty: CTMT propagates uncertainty only along supported curvature directions. Redundant directions are inert with respect to both distinguishability and uncertainty growth.

F. Comparison to synthetic ground truth

The ground-truth information geometry of the model (11) is one-dimensional: all observable distributions live on a one-parameter family indexed by $\theta_1 + \varepsilon\theta_2$. CTMT reconstruction yields:

- **Correct dimensionality:** the rank-one Fisher spectrum implies a one-dimensional coherent subspace.
- **Correct causal ordering:** coherence proper time τ is monotonic and independent of redundant coordinates.
- **Correct uncertainty scale:** $\mathrm{Var}(\Phi) = k^2\sigma^2$ matches the underlying Gaussian noise.
- **Redundancy rejection:** the θ_2 channel is identified as Fisher-null and excluded from coherent transport.

No parameter tuning, regularization, or external structure is required.

G. Malformed spectra and CRSC

In this toy model, F remains exactly rank one for any ε, with a single nonzero eigenvalue. In realistic systems, however, strong contamination or poorly constrained parameters generically produce Fisher spectra with clusters of small eigenvalues and reduced coherence density. Such spectra violate the Coherence–Redundancy Stabilization Criterion (CRSC): the system cannot maintain a stable separation between coherent and redundant directions.

In CTMT this triggers an enforced rank collapse of the effective geometry: only the robustly supported directions survive as part of the coherent causal structure, while ill-conditioned directions are discarded as causally unstable.

H. Main theorem

The above construction illustrates a special case of the following general statement.

Theorem A.1 (Constructive operability of CTMT)**.** *Let a finite statistical model admit a positive semidefinite Fisher information tensor F. Then CTMT reconstructs:*

1) *the maximal coherent subspace of the parameter manifold, defined by the support of the nonzero Fisher spectrum;*
2) *a coherence proper time functional defining a causal ordering along information-bearing directions;*
3) *an uncertainty propagation law restricted to non-null directions of Fisher curvature,*

using only the spectral geometry of F. Redundant or malformed directions are identified as null or unstable curvature directions and do not contribute to coherent causal transport.

Proof. Positive semidefiniteness of F guarantees an orthogonal decomposition into eigenspaces with nonnegative eigenvalues. The span of eigenvectors with nonzero eigenvalues defines the maximal coherent subspace: only displacements within this subspace change the observable distribution. Coherence proper time is defined as a monotonic functional of $\lambda_{\max}(F)$ along trajectories in this subspace, ensuring a well-defined causal ordering.

Uncertainty propagation in CTMT is expressed via the Moore–Penrose inverse F^+, which by construction acts as the inverse of F on the coherent subspace and annihilates null directions. Consequently, only non-null directions contribute to propagated variance, while redundant directions have no effect on distinguishability, causality, or uncertainty. Directions associated with unstable, clustered, or vanishing eigenvalues violate CRSC and are excluded from the coherent geometry by the same spectral mechanism. □

I. Corollaries

Corollary A.2 (Noise robustness)**.** *CTMT correctly propagates uncertainty and preserves causal ordering under additive noise and weak parameter corruption, as long as the Fisher tensor remains positive semidefinite with a well-separated nonzero spectrum.*

Corollary A.3 (Automatic redundancy detection)**.** *Any parameter direction that does not affect observables is geometrically identified as a null direction of Fisher curvature and is excluded from the coherent causal structure without additional postulates.*

Corollary A.4 (Non-arbitrariness of geometry)**.** *CTMT introduces no arbitrary choices of metric, dimension, or gauge structure. All effective geometry, including coherent dimensionality and causal ordering, is forced by the information geometry of F together with coherence constraints such as CRSC.*

J. Time-dependent Fisher manifold with perturbed redundancy

The static example above can be extended to a time-dependent Fisher manifold in which a previously redundant direction acquires a small but nonzero curvature eigenvalue. This allows us to examine how CTMT treats weakly informative perturbations and how this affects forward-prediction accuracy.

1) Time-dependent statistical model: Let $t \in [0, T]$ be a label for successive observation epochs and consider

$$p\big(x \mid \theta_1(t), \theta_2(t)\big) = \mathcal{N}\big(x \;\big|\; \theta_1(t) + \varepsilon(t)\,\theta_2(t),\ \sigma^2\big)\,, \quad (22)$$

with:

- $\theta_1(t)$ the primary signal parameter,
- $\theta_2(t)$ a secondary control channel,
- $\varepsilon(t)$ a time-dependent contamination factor,
- σ^2 fixed observational noise as before.

We assume that for early times $\varepsilon(t)$ is very small, while at later times it grows to a small but non-negligible value:

$$\varepsilon(t) = \varepsilon_0 + \delta\varepsilon(t), \qquad 0 < \varepsilon_0 \ll 1, \qquad |\delta\varepsilon(t)| \lesssim \varepsilon_0, \quad (23)$$

so that the second parameter direction becomes weakly informative but remains subdominant.

2) Time-dependent Fisher tensor and spectrum: The Fisher information at time t has the same analytic form as (15) with ε replaced by $\varepsilon(t)$:

$$F(t) = \frac{1}{\sigma^2}\begin{pmatrix} 1 & \varepsilon(t) \\ \varepsilon(t) & \varepsilon^2(t) \end{pmatrix}. \tag{24}$$

The eigenvalues of $F(t)$ are

$$\lambda_{\max}(t) = \frac{1+\varepsilon^2(t)}{\sigma^2}, \qquad \lambda_{\min}(t) = 0, \tag{25}$$

exactly as before. To model a genuinely weakly informative second direction, we perturb the model slightly by adding a small independent contribution to the variance along θ_2:

$$F_\delta(t) = \frac{1}{\sigma^2}\begin{pmatrix} 1 & \varepsilon(t) \\ \varepsilon(t) & \varepsilon^2(t) \end{pmatrix} + \delta(t)\begin{pmatrix} 0 & 0 \\ 0 & 1 \end{pmatrix}, \qquad 0 < \delta(t) \ll \frac{1}{\sigma^2}. \tag{26}$$

Now the eigenvalues become

$$\lambda_{\max}(t) = \frac{1+\varepsilon^2(t)}{\sigma^2} + O\big(\delta(t)\big), \tag{27}$$

$$\lambda_{\min}(t) = \delta(t) + O\big(\varepsilon^2(t)\,\delta(t)\big), \tag{28}$$

so that the second direction carries a small but nonzero amount of Fisher curvature. The ratio

$$r(t) = \frac{\lambda_{\min}(t)}{\lambda_{\max}(t)} \approx \delta(t)\,\sigma^2 \tag{29}$$

serves as a dimensionless measure of how informative the second direction is relative to the dominant one.

3) Coherence proper time and causal ordering: Coherence proper time along a trajectory is now

$$\tau(t) = \int_0^t \sqrt{\lambda_{\max}\big(F_\delta(t')\big)}\,dt' \approx \int_0^t \frac{\sqrt{1+\varepsilon^2(t')}}{\sigma}\,dt', \tag{30}$$

since $\delta(t)$ enters only as a small correction to the largest eigenvalue.

As long as $r(t) \ll 1$ for all t in the interval of interest,

- $\lambda_{\max}(t)$ remains dominated by the primary direction,
- $\tau(t)$ remains strictly monotonic,
- causal ordering is essentially unchanged by the weakly informative second direction.

Only when $r(t)$ approaches order one does the second direction significantly modify the coherence-time ordering, signaling a transition in the effective geometry.

4) Two reconstruction schemes and prediction accuracy: To compare the impact of including the weakly informative direction, consider two reconstruction schemes:

Scheme A (CTMT-trimmed). Use only the dominant eigen-direction of $F_\delta(t)$ when $r(t) < r_*$, for some small threshold r_* imposed by CRSC. The effective model is one-dimensional, with parameters projected onto the principal direction. The second direction is treated as redundant noise for purposes of coherent transport and uncertainty propagation.

Scheme B (full-parameter). Use both eigen-directions of $F_\delta(t)$ for reconstruction and forward prediction, regardless of the size of $r(t)$. The effective model is two-dimensional, and uncertainty is propagated in both directions.

Let Φ_t denote an observable derived from $(\theta_1(t), \theta_2(t))$, such as a predicted mean $\theta_1(t) + \varepsilon(t)\theta_2(t)$ or a more complex functional. Let $\widehat{\Phi}_t^{(A)}$ and $\widehat{\Phi}_t^{(B)}$ be the respective predictions under Schemes A and B, and let Φ_t^{true} be the ground-truth observable.

Define a mean-square prediction error over an observation window $[0, T]$:

$$E_A = \frac{1}{T}\int_0^T \big(\widehat{\Phi}_t^{(A)} - \Phi_t^{\mathrm{true}}\big)^2 dt, \qquad E_B = \frac{1}{T}\int_0^T \big(\widehat{\Phi}_t^{(B)} - \Phi_t^{\mathrm{true}}\big)^2 dt. \tag{31}$$

a) CTMT prediction.:

- When $r(t) \ll r_*$ for all t (second direction extremely weak), Scheme A is expected to achieve *lower* or comparable error $E_A \lesssim E_B$, because it avoids injecting spurious degrees of freedom and propagating noise in nearly null directions.
- As $r(t)$ increases and approaches r_*, the curvature carried by the second direction becomes non-negligible. CTMT predicts a transition region where including the second direction begins to improve accuracy: for $r(t) \gtrsim r_*$ on a substantial portion of the interval, one expects $E_B \lesssim E_A$.
- If $r(t)$ fluctuates, CTMT provides a principled switching criterion: use Scheme A where $r(t) < r_*$ and Scheme B where $r(t) \geq r_*$, maintaining causal ordering in τ while incorporating genuinely informative directions.

In all cases, coherence proper time is defined by $\lambda_{\max}(t)$ and remains monotonic; the role of $\lambda_{\min}(t)$ is to determine whether the second direction participates in the coherent geometry or is relegated to redundancy.

5) Interpretation: This time-dependent, weakly perturbed example illustrates a key feature of CTMT:

- **Geometry is adaptive:** the effective dimension of the coherent manifold is not fixed but responds to the Fisher spectrum via CRSC.
- **Causality is stable:** coherence-time ordering is controlled by $\lambda_{\max}(t)$ and remains robust to small perturbations in subdominant directions.
- **Predictive accuracy is spectrum-driven:** including a weakly informative direction only improves forward prediction once its curvature weight $r(t)$ exceeds a coherence threshold. Below that threshold, geometric trimming (Scheme A) yields cleaner, more stable predictions.

Thus, CTMT not only extracts coherent geometry and causal structure from time-dependent Fisher manifolds, but also provides a principled mechanism for deciding when additional parameters become genuinely predictive rather than serving as redundant noise.

K. Significance

This construction demonstrates that CTMT is a mathematically operational framework capable of extracting geometry, causality, and uncertainty structure from finite, imperfect models using only Fisher spectral data. It does not rely on physical assumptions and is directly applicable to inference, control, and engineering systems, as well as to the physical applications discussed in the main text.

REFERENCES

[1] S. Amari and H. Nagaoka, *Methods of Information Geometry*, AMS, 2000.

[2] N. Ay, J. Jost, H. Lê, and L. Schwachhöfer, *Information Geometry*, Springer, 2017.

[3] L. Bombelli, J. Lee, D. Meyer, and R. Sorkin, "Spacetime as a causal set," Phys. Rev. Lett. **59**, 521 (1987).

[4] L. Hardy, "Towards quantum gravity: a framework for probabilistic theories with non-fixed causal structure," J. Phys. A **40**, 3081 (2007).

[5] H.-P. Breuer and F. Petruccione, *The Theory of Open Quantum Systems*, Oxford University Press, 2002.

[6] T. Jacobson, "Thermodynamics of spacetime: The Einstein equation of state," Phys. Rev. Lett. **75**, 1260 (1995).